

Preparation and Conformational Properties of the Perfluoro Diether $\text{CF}_3\text{OCF}_2\text{OCF}_2\text{C}(\text{O})\text{F}$, a Model Molecule to Study Properties of Perfluoro Polyethers

R. M. Romano,^{†,‡} J. Czarnowski,^{‡,§} and C. O. Della Védova^{*,†,‡,||}

CEQUINOR (CONICET-UNLP) and Laboratorio de Servicios a la Industria y al Sistema Científico (UNLP-CIC-CONICET), Departamento de Química, Facultad de Ciencias Exactas, Universidad Nacional de La Plata, 47 esq. 115, (1900) La Plata, Argentina, and Instituto de Investigaciones Físicoquímicas Teóricas y Aplicadas, Sucursal 4, Casilla de Correo 16, (1900) La Plata, Argentina

Received July 31, 2000

The compound $\text{CF}_3\text{OCF}_2\text{OCF}_2\text{C}(\text{O})\text{F}$ was prepared by oxidation of hexafluoropropene with molecular oxygen in the gas-phase using CF_3OF as initiator. ^{13}C NMR, FTIR, Raman, UV–vis, and mass spectra were obtained and interpreted. The theoretical structure studies were performed by the calculation of the potential energy surfaces, using the results obtained for a smaller related molecule, $\text{CF}_3\text{OCF}_2\text{C}(\text{O})\text{F}$, as a starting point. A high degree of conformational flexibility of this compound is evidenced by the values of several conformations, varying within the range of 1 kcal/mol. Theoretical calculations predict chain conformations as the most stable molecular forms, as expected from the presence of the anomeric effect. The experimental fundamental vibrational modes are compared with those obtained theoretically, using *ab initio* and density functional theory methods, HF/6-31+G* and B3LYP/6-31+G*, respectively. The density of the compound at ambient temperature ($\delta = 1.7(1)$ g/mL), its melting point (mp = $-140(5)$ °C), its boiling point (bp = $14.5(1)$ °C), and the relation between its vapor pressure and the absolute temperature ($\ln P = 13.699 - 2023.4/T$) were also determined.

Introduction

In recent years there has been an increase of interest in the chemistry of fluorine-containing compounds, especially with regard to the development of new fluoropharmaceuticals, agrochemicals, and fluoropolymers. There is now hardly an area of chemistry and biochemistry where fluorine chemistry does not have a significant impact. Synthetic fluorine chemistry is becoming of increasing interest to organic and inorganic chemists.

The chemistry of fluorine is different from that of other halogens because of a low dissociation energy of the fluorine molecule (37.5 kcal/mol), a relatively high strength of bonds formed between fluorine and metallic or nonmetallic elements, and a relatively small size of fluorine atom and its fluoride ion.

The substitution of hydrogen by fluorine atoms is widely used for synthetic purposes in many areas of chemistry and biochemistry. However, the assumption that the substituting fluorine atom can act similarly to the hydrogen atom may be misleading. The comparison between the van der Waals radii ($r_{\text{F}} = 1.47$ Å, $r_{\text{O}} = 1.57$ Å, $r_{\text{H}} = 1.20$ Å and $E_{\text{F}} = 4$, $E_{\text{O}} = 3.5$, $E_{\text{H}} = 2.1$), indicates that the size of the fluorine atom is only slightly smaller than that of the oxygen atom but it is larger than that of the hydrogen atom. The size of CF_3 group is 2 or 3 times larger than that of the CH_3 group, the former being comparable to the size of the isopropyl group. Nevertheless, it is usually accepted that the replacement of CH_3 by CF_3 group in a molecule does not affect significantly its conformation.

The substitution of a methyl group, attached to the carbon atom, by a trifluoromethyl group does not change substantially the length of the C–C bond. However, the replacement of hydrogen atoms adjacent to the carbon atoms by fluorine atoms increases the C–C bond strength making the molecule more stable. In addition, this substitution may lead to electronic changes associated with the anomeric effect when the atom bonded to a CF moiety has one or more lone pairs of electrons.

The photooxidation of perfluoroolefins (CF_2CF_2 , CF_3CFCF_2) in liquid phase^{1–6} at 233 K or lower, initiated by ultraviolet light, is one of the major routes utilized for commercial production of fluid perfluoro polyethers, high-performance lubricants for aerospace and industrial applications. Nowadays they are also used as lubricants for magnetic hard disks in computers, because of their good performance as a protective layer between the hard disk surface and the magnetic head. These lubricants are mixtures of different molecular mass species containing $\text{CF}_2\text{—O}$ groups in their main chains with interesting physical–chemical features such as low vapor pressure, wide liquid-temperature range, and chemical inertness.

It was reported⁷ that, in the gas-phase photooxidation of hexafluoropropene at 303 K, the main reaction product was a

[†] CEQUINOR.

[‡] Postdoctoral (R.M.R.) and Member of the Carrera del Investigador Científico (J.C. and C.O.D.V.) of the Consejo Nacional de Investigaciones Científicas y Técnicas de Argentina.

[§] Instituto de Investigaciones Físicoquímicas Teóricas y Aplicadas.

^{||} Laboratorio de Servicios a la Industria y al Sistema Científico.

- (1) Sianesi, D. *ACS Polym. Prepr.* **1971**, *12*, 411–419.
- (2) Fautitano, A.; Buttafava, A.; Comincioli, V.; Marchionni, G.; De Pasquale, R. J. *J. Phys. Org. Chem.* **1991**, *4*, 293–300.
- (3) Sianesi, D.; Marchionni, G.; De Pasquale, R. J. *Organic Fluorine Chemistry: Principles and Commercial Applications*; Banks, R. E., Smart, B. E., Tatlow, J. C., Eds.; Plenum Press: New York, 1994; pp 431–461.
- (4) Sianesi, D.; Guarda, P. A.; Marchionni, G. *Macromolecules* **1999**, *32*, 7768–7780.
- (5) Bunyard, W. C.; Romack, T. J.; DeSimone, J. M. *Macromolecules* **1999**, *32*, 8224–8226.
- (6) Malavasi M.; Sianesi, D. *J. Fluorine Chem.* **1999**, *95*, 19–25.
- (7) Sianesi D.; Pasetti A.; Fontanelli R.; Bernardi G. C.; Caporiccio G., *Chim. Ind.* **1973**, *55*, 208–221.

mixture of two series of telomers, $\text{CF}_3\text{O}(\text{CF}_2\text{O})_n\text{C}(\text{O})\text{F}$ and $\text{CF}_3\text{O}(\text{CF}_2\text{O})_n\text{CF}_2\text{C}(\text{O})\text{F}$, where $n = 1 \rightarrow 12$.

The chemical initiators can lead to the selective synthesis of perfluoro polyether molecules of lower relative molecular mass thus providing useful tools for the studies of the unique properties of perfluoro polyethers attributed to their different segments and end groups, using a simple molecule.

The stable and easily handled (trifluoromethyl)hypofluorite, CF_3OF , containing a weak O–F bond (43.5 kcal/mol),^{8–10} is an effective initiator.

Recently we have studied the kinetic and mechanistic aspects of the thermal oxidation of hexafluoropropene with molecular oxygen in the gas phase and in the temperature range of 303.0–323.4 K, using CF_3OF as initiator.¹¹ The product of highest molecular mass obtained was tentatively assigned the structure $\text{CF}_3\text{OCF}_2\text{OCF}_2\text{C}(\text{O})\text{F}$ on the basis of its relative mass determination and by comparison of the observed infrared bands frequencies with those predicted theoretically by the preliminary calculations corresponding to the proposed structure.

Despite the industrial importance of perfluoro polyethers, little is known about their structure and spectroscopic properties. The study of molecular geometry in $\text{CF}_3\text{OCF}_2\text{CF}_3$ ¹² and the structural studies¹³ on CF_3OCF_3 , $\text{CF}_3\text{OCF}(\text{CF}_3)\text{CF}_2\text{OCF}_3$, and $\text{CF}_3\text{CF}_2\text{OCF}(\text{CF}_3)\text{CF}_2\text{OCF}_2\text{CF}_3$ were reported in the literature.

The insight into the energy-minimum structure and conformation energy map of C–C, C–O, C–O–C, and C–C–O bonds, present in small as well as in larger molecules of perfluoro polyethers, provides information about the most probable sites of specific bond fissions, allowing predicting the relative probability of the elementary reactions to occur during the oxidation process. This could offer an additional guide to the technology that is already engaged in commercial production of these chemicals, considered as the most advanced and successful products in fluorine chemistry.

The perfluoro diether $\text{CF}_3\text{OCF}_2\text{OCF}_2\text{C}(\text{O})\text{F}$ is expected to be useful as a model compound for the study of physicochemical and thermodynamical properties of the more complex perfluoro polyethers, components of the lubricants, contributing to elucidate the structure–properties correlation.

$\text{CF}_3\text{OCF}_2\text{OCF}_2\text{C}(\text{O})\text{F}$, due to its chemical inertness, could be also a useful alternative refrigerant, because of usually excellent vaporization properties of perfluorinated compounds containing oxygen atoms. However, its atmospheric lifetime should be very long, thus contributing, given its infrared absorption characteristics, to the global warming potential.

In this work a thorough calculation of IR spectrum of $\text{CF}_3\text{OCF}_2\text{OCF}_2\text{C}(\text{O})\text{F}$, using HF/6-31+G* ab initio and B3LYP/6-31+G* and B3PW91/6-31+G* functional theory methods, has been undertaken and the complete vibrational analysis performed. In addition to this, the NMR, Raman, UV–vis, and mass spectra were carried out and interpreted to support the identification of the compound. The density of the compound at ambient temperature, the melting and boiling points, and the relation between its vapor pressure and the absolute temperature were determined.

Experimental Section

$\text{CF}_3\text{OCF}_2\text{OCF}_2\text{C}(\text{O})\text{F}$ was prepared by the gas-phase thermal oxidation of C_3F_6 by O_2 , using CF_3OF as initiator.¹¹ All reactants were purchased commercially. CF_3OF (PCR, 97–98%) was washed with 0.1 mol dm^{-3} NaOH solution and filtered at 80 K. C_3F_6 (PCR, 97–98%) was purified by repeated low-pressure trap-to-trap distillations on a vacuum line, the middle fraction being retained each time. O_2 (La Oxigena, 99.99%) and N_2 (La Oxigena, 99.9%) were bubbled through 98% analytical-grade H_2SO_4 and passed slowly through a Pyrex coil at 123 K and at liquid air temperature, respectively. A total of 14 runs were made at 324 K in a spherical quartz bulb of 270 cm^3 . The initial pressure of CF_3OF varied between 1.6 and 4.0 Torr, that of C_3F_6 between 107 and 169 Torr, and that of O_2 between 170 and 240 Torr. The experiments were carried out to the total consumption of C_3F_6 . Each time $\text{CF}_3\text{OCF}_2\text{OCF}_2\text{C}(\text{O})\text{F}$ was separated as a residue at 163 K by fractional condensation and all residues were collected together in a trap at liquid air temperature. The $\text{CF}_3\text{OCF}_2\text{OCF}_2\text{C}(\text{O})\text{F}$ yields were 35% based on the initial pressure of C_3F_6 . In these experimental conditions explosion occurred at initial pressures of CF_3OF and C_3F_6 greater than 4.0 and 190 Torr, respectively.

$\text{CF}_3\text{OCF}_2\text{OCF}_2\text{C}(\text{O})\text{F}$ is colorless in the gas and liquid phase and glassy in the solid state. The density of the compound at ambient temperature is $\delta = 1.7(1)$ g/mL. The compound shows a wide liquid-temperature range of about 154.5 °C, an expected behavior for this class of compounds. A melting point of mp = –140(5) °C, a boiling point of bp = 14.5(1) °C, and a relation between its vapor pressure and the absolute temperature of $\ln P = 13.699 - 2023.4/T$ were determined.

A Bruker IFS66 instrument was used to record the gas FTIR spectra between 4000 and 400 cm^{-1} at 2 and 40 Torr and room temperature using 10-cm cells provided with KBr windows. The resolution was 1 cm^{-1} . Raman spectra of the liquid between 2000 and 100 cm^{-1} were obtained with a Spex Ramalog spectrometer (spectral resolution of 5 cm^{-1}). An Ar laser (Spectra-Physics model 165) providing the 514.5 nm excitation line was used, with a power of 40 and 200 mW. The measurements were performed in a glass low-temperature cell at 185 K. The UV–vis spectrum was recorded in the gas phase at 5 Torr using a Perkin-Elmer 9 UV spectrophotometer with a quartz cell and optical path of 10 cm.

The mass spectrum was taken with a Trio-2 spectrometer with 3000 units of atomic mass provided by Micromass, Manchester, U.K. Ionization energies of 20 and 70 eV were applied.

¹³C NMR spectra were obtained with an AC 250 MHz Bruker instrument. The data were referenced to the solvent CDCl_3 . The δ values for the title compounds are the following: 147.2 (td, ¹J(CF) = 374 Hz, ²J(CF) = 46 Hz, C(O)F); 118.8 (q, ¹J(CF) = 268 Hz, CF₃); 117.9 (t, ¹J(CF) = 274 Hz, OCF₂*); 117.7 (t, ¹J(CF) = 275 Hz, OCF₂*).

The ab initio and density functional theory calculations were performed using the Gaussian 98 program package¹⁴ under the Linda parallel execution environment.

Theoretical Calculations

The structure of the $\text{CF}_3\text{OCF}_2\text{OCF}_2\text{C}(\text{O})\text{F}$ was hitherto unknown. To study its structure from a theoretical point of view it is necessary to find the minima of the potential energy surfaces originated by the variation of the different torsional angles. The skeleton of $\text{CF}_3\text{OCF}_2\text{OCF}_2\text{C}(\text{O})\text{F}$ possesses five independent

(8) Czarnowski, J.; Castellano, E.; Schumacher, H. J. *Z. Phys. Chem. (Munich)* **1969**, *65*, 225–237.

(9) Czarnowski, J.; Schumacher, H. J. *Z. Phys. Chem. (Munich)* **1970**, *78*, 68–76.

(10) Kennedy, R. C.; Levy, J. B. *J. Phys. Chem.* **1972**, *76*, 3480–3488.

(11) dos Santos Afonso, M.; Romano, R. M.; Della Védova, C. O.; Czarnowski, J. *Phys. Chem. Chem. Phys.* **2000**, *2*, 1393–1399.

(12) Stanton, C. L.; Paige, H. L.; Schwartz, M. J. *Phys. Chem.* **1993**, *97*, 5901–5904.

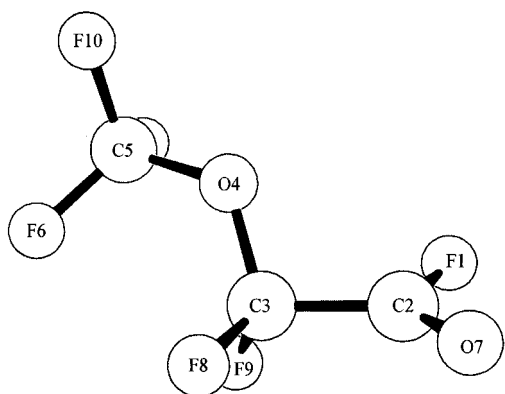
(13) Pacansky, J.; Liu, B. *J. Phys. Chem.* **1985**, *89*, 1883–1887.

(14) Frisch, M. J.; Trucks, G. W.; Schlegel, H. B.; Scuseria, G. E.; Robb, M. A.; Cheeseman, J. R.; Zakrzewski, V. G.; Montgomery, J. A., Jr.; Stratmann, R. E.; Burant, J. C.; Dapprich, S.; Millam, J. M.; Daniels, A. D.; Kudin, K. N.; Strain, M. C.; Farkas, O.; Tomasi, J.; Barone, V.; Cossi, M.; Cammi, R.; Mennucci, B.; Pomelli, C.; Adamo, C.; Clifford, S.; Ochterski, J.; Petersson, G. A.; Ayala, P. Y.; Cui, Q.; Morokuma, K.; Malick, D. K.; Rabuck, A. D.; Raghavachari, K.; Foresman, J. B.; Cioslowski, J.; Ortiz, J. V.; Baboul, A. G.; Stefanov, B. B.; Liu, G.; Liashenko, A.; Piskorz, P.; Komaromi, I.; Gomperts, R.; Martin, R. L.; Fox, D. J.; Keith, T.; Al-Laham, M. A.; Peng, C. Y.; Nanayakkara, A.; Gonzalez, C.; Challacombe, M.; Gill, P. M. W.; Johnson, B.; Chen, W.; Wong, M. W.; Andres, J. L.; Gonzalez, C.; Head-Gordon, M.; Replogle, E. S.; Pople, J. A. *Gaussian 98 (Revision A.7)*; Gaussian, Inc.: Pittsburgh, PA, 1998.

Table 1. Relative Energies and Torsional Angles of the Stable Conformers of CF₃OCF₂C(O)F Calculated with Different Theoretical Approximations^a

conformer	HF/3-21G *		HF/6-31+ G*		B3LYP/6- 31+G*		B3PW91/ 6-31+G*	
	ΔE (kcal/mol)	torsional angles (deg)	ΔE (kcal/mol)	torsional angles (deg)	ΔE (kcal/mol)	torsional angles (deg)	ΔE (kcal/mol)	torsional angles (deg)
1	0.00	$\tau_1 = -65$ $\tau_2 = 164$ $\tau_3 = 28$	0.00	$\tau_1 = -65$ $\tau_2 = 162$ $\tau_3 = 42$	0.00	$\tau_1 = -64$ $\tau_2 = 165$ $\tau_3 = 44$	0.00	$\tau_1 = -63$ $\tau_2 = 164$ $\tau_3 = 44$
2	0.88	$\tau_1 = 175$ $\tau_2 = 164$ $\tau_3 = 28$	0.46	$\tau_1 = 178$ $\tau_2 = 163$ $\tau_3 = 42$	0.17	$\tau_1 = 179$ $\tau_2 = 166$ $\tau_3 = 45$	0.17	$\tau_1 = 178$ $\tau_2 = 165$ $\tau_3 = 44$
3	2.03	$\tau_1 = 178$ $\tau_2 = 84$ $\tau_3 = -33$	1.14	$\tau_1 = -177$ $\tau_2 = 87$ $\tau_3 = -40$	0.87	$\tau_1 = -172$ $\tau_2 = 84$ $\tau_3 = -39$	0.83	$\tau_1 = -170$ $\tau_2 = 83$ $\tau_3 = -39$
4	2.25	$\tau_1 = 39$ $\tau_2 = 67$ $\tau_3 = -34$	1.16	$\tau_1 = 49$ $\tau_2 = 75$ $\tau_3 = -44$	0.58	$\tau_1 = 49$ $\tau_2 = 71$ $\tau_3 = 45$	0.55	$\tau_1 = 48$ $\tau_2 = 71$ $\tau_3 = -45$
5	3.60	$\tau_1 = -55$ $\tau_2 = 71$ $\tau_3 = 21$	1.14	$\tau_1 = -177$ $\tau_2 = 87$ $\tau_3 = 80$	0.86	$\tau_1 = -171$ $\tau_2 = 83$ $\tau_3 = 82$	0.83	$\tau_1 = -170$ $\tau_2 = 83$ $\tau_3 = 82$

^a $\tau_1 = \text{F1C2C3O4}$, $\tau_2 = \text{C2C3O4C5}$, and $\tau_3 = \text{C3O4C5F6}$.

**Figure 1.** Molecular model of CF₃OCF₂C(O)F predicted considering the anomeric effect, which reveals the chain structure.

torsions, making the analysis not only difficult but also very time-consuming. For this reason, we started the theoretical study using a smaller related molecule, CF₃OCF₂C(O)F. This compound provides a good opportunity to study the influence of the anomeric effect on the conformation adopted by the molecule. The generalized anomeric effect¹⁵ may affect significantly the conformational properties of a molecule. The origin of this stereoelectronic effect, in the case of perfluorinated ethers, is the orbital interaction between a p lone pair orbital at oxygen atom and the σ^* orbital of the opposite C–F bond, making operative the two π bonds from each CF₂ and CF₃ moieties. According to this interaction a chain structure, illustrated in the Figure 1, can be predicted for the molecule containing ether functions. The conformational uncertainty would result from the orientation of the C(O)F group, with respect to the OCF₂ group, directly linked to the former group.

The CF₃OCF₂C(O)F molecule has three independent torsions: $\tau_1(\text{F1C2C3O4})$, $\tau_2(\text{C2C3O4C5})$, and $\tau_3(\text{C3O4C5F6})$ (see Figure 1). Three different potential energy surfaces were calculated for three different values of $\tau_1(\text{F1C2C3O4})$, 0° (cis), 90° (gauche), and 180° (trans), using the HF/3-21G* approximation, by varying the values of $\tau_2(\text{C2C3O4C5})$ between 0 and 360° at intervals of 30° and those of $\tau_3(\text{C3O4C5F6})$ between 0 and 120° at intervals of 10°, with geometry optimization at each point on the surfaces. Figure 2 shows the

calculated potential energy surfaces. The 26 minima, found over these three surfaces, were fully optimized using the HF/3-21G* approximation, with the simultaneous relaxation of all the geometrical parameters. The vibrational wavenumbers were calculated to characterize the stationary points as minima. After this optimization there were only five possible structures left, because all others structures have been converted to the corresponding five minima by the relaxation of the fixed torsional angles. These five structures were subsequently fully optimized using the HF/6-31+G*, B3LYP/6-31+G*, and B3PW91/6-31+G* levels of the theory. Table 1 lists the energy differences and the calculated torsional angles for these five structures, and Figure 3 illustrates their conformations. In all cases the vibrational calculations correspond to the minima for which no imaginary wavenumbers occur. Structure **5** converges to structure **3** with the HF/6-31+G*, B3LYP/6-31+G*, and B3PW91/6-31+G* models, leaving only four different structures. These four forms can be described as gauche-trans (F1–C2 gauche with respect to C3–O4 and C2–C3 trans with respect to O4–C5), trans-trans, gauche-gauche, and trans-gauche, following the order of increasing energy. These theoretical results are in agreement with those expected from the consideration of the anomeric effect. Conformers **1** and **2** are structures in which the anomeric effect is maximized. Both differ only in the relative position of the FC(O) group. Conformers **3** and **4** are comparable between themselves and have higher energy than the conformers **1** and **2**. Only one of the fluorine atoms of the CF₂ group can interact with the lone pairs at the oxygen atom to promote the anomeric effect. In the conformer **5**, the highest calculated with the HF/3-21G* approximation, the anomeric contribution from the fluorine atom of the CF₃ group disappears.

As the atomic relative position would not be affected by the incorporation of the CF₂O group into the molecule, conformers **1** and **2** were further used to calculate the structure of CF₃OCF₂OCF₂C(O)F. For this molecule there are five independent torsions: $\tau_1(\text{F1C2C3O4})$; $\tau_2(\text{C2C3O4C5})$; $\tau_3(\text{C3O4C5O6})$; $\tau_4(\text{O4C5O6C7})$; $\tau_5(\text{C5O6C7F8})$. The theoretical analysis was made by assuming that the values of the torsional angles $\tau_1(\text{F1C2C3O4})$, $\tau_2(\text{C2C3O4C5})$, and $\tau_5(\text{C5O6C7F8})$ remain the same as in the smaller related molecule CF₃OCF₂C(O)F. The potential energy surfaces were calculated for the variation of the other two torsions, $\tau_3(\text{C3O4C5O6})$ and $\tau_4(\text{O4C5O6C7})$, between 0 and 360° at intervals of 30°, for the gauche and trans

(15) Kirby, A. J. *The Anomeric Effect and Related Stereoelectronic Effects at Oxygen*; Springer-Verlag: Berlin, 1983.

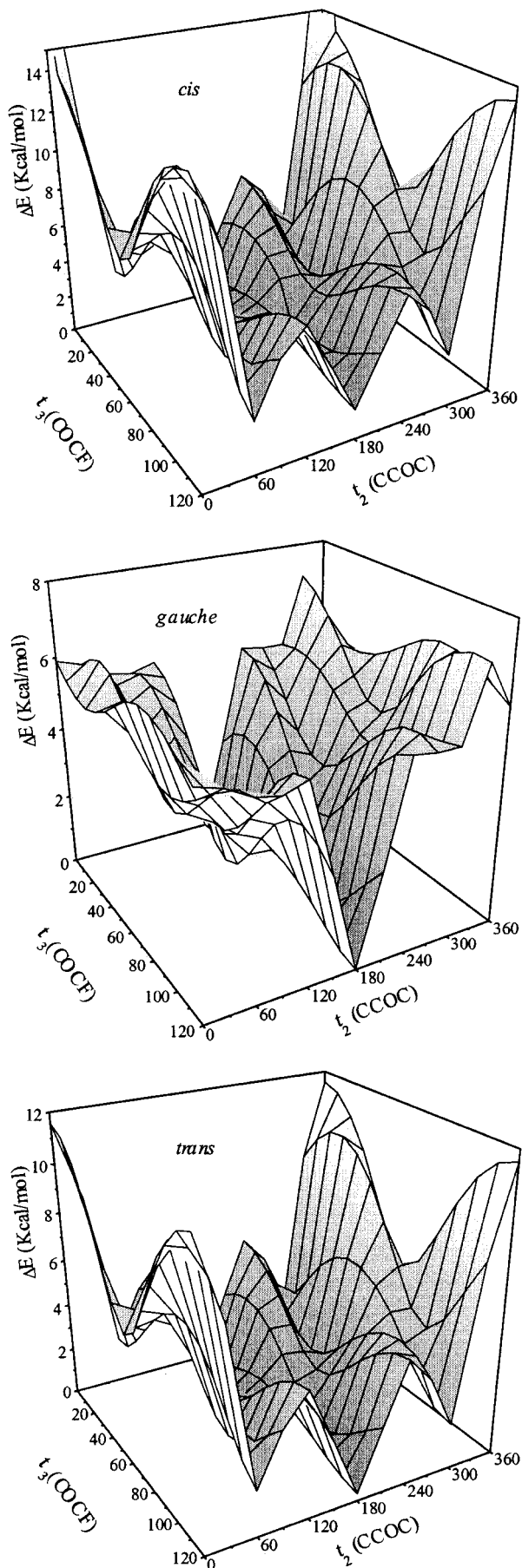


Figure 2. Potential energy surfaces of $\text{CF}_3\text{OCF}_2\text{C}(\text{O})\text{F}$ calculated with the HF/3-21G* approximation for three different values of τ_1 - (F1C2C3O4): 0° (cis); 90° (gauche); 180° (trans).

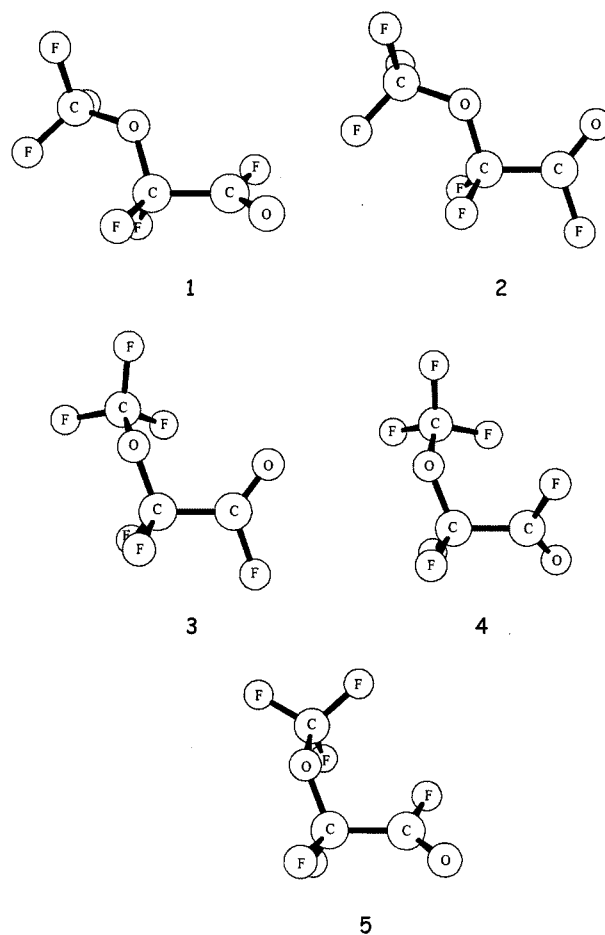


Figure 3. HF/3-21G* calculated structures of $\text{CF}_3\text{OCF}_2\text{C}(\text{O})\text{F}$.

conformers. Each point on these surfaces was calculated by the optimization of the geometric parameters, with exception of the considered torsions. Figure 4 shows the potential energy surfaces for the gauche and trans conformers. The analysis of these surfaces reveals the presence of 15 minima, 7 for the gauche conformer and 8 for the trans conformer. These 15 minima were subsequently optimized using the HF/3-21G*, HF/6-31+G*, and B3LYP/6-31+G* approximations, by simultaneous relaxation of all the geometrical parameters. Table 2 lists the relative energies and the calculated torsional angles of the stable conformers of $\text{CF}_3\text{OCF}_2\text{OCF}_2\text{C}(\text{O})\text{F}$. All conformations constitute minima in the potential hyper surface with no imaginary wavenumbers. These calculations show the high conformational flexibility associated with this molecule. Most of the 15 conformers calculated in Table 2 are in the range of 1 kcal/mol. The described situation can be also appreciated by inspection of the Figure 4. The high conformational flexibility is crucial for the application of this type of compounds as a protective layer between the magnetic hard disk surface and the magnetic head.

Figure 5 illustrates the most stable conformations of this molecule as calculated by HF/6-31+G* and B3LYP/6-31+G* levels of approximation, and Table 3 lists the calculated geometrical parameters. The structures confirm the conformational behavior as expected from the influence of the anomeric effect.

Vibrational Analysis

Figures 6 and 7 show the gas FTIR and the liquid Raman spectra of $\text{CF}_3\text{OCF}_2\text{OCF}_2\text{C}(\text{O})\text{F}$. The observed wavenumbers,

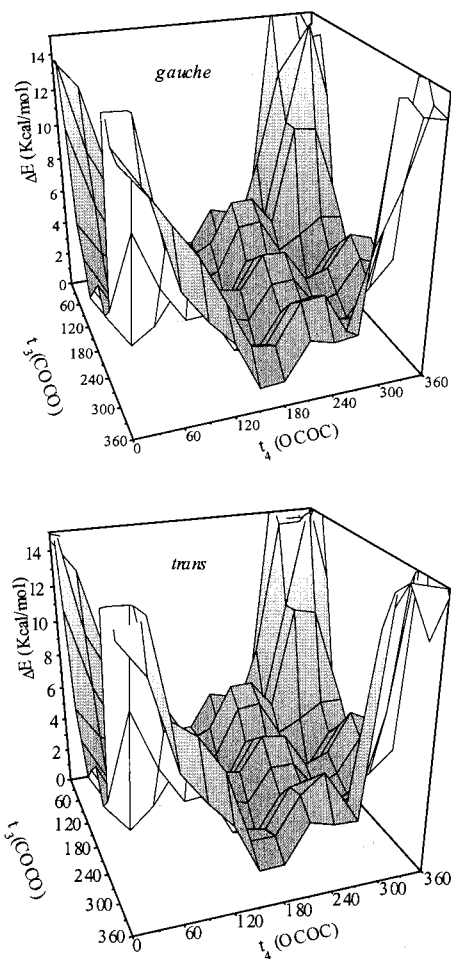


Figure 4. Potential energy surfaces of $\text{CF}_3\text{OCF}_2\text{OCF}_2\text{C(O)F}$ calculated with the HF/3-21G* approximation for the gauche and trans conformers.

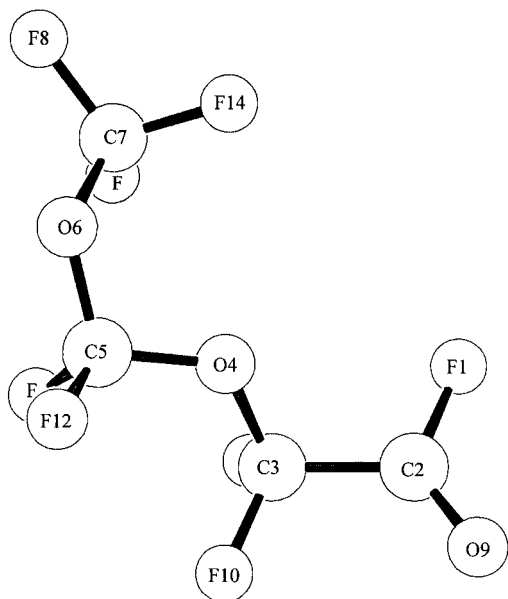


Figure 5. B3LYP/6-31+G* calculated structure of $\text{CF}_3\text{OCF}_2\text{OCF}_2\text{C(O)F}$.

together with a tentative assignment and theoretical wavenumbers for the most stable conformer, are listed in Table 4. The results obtained with the HF methods were scaled by a 0.9 factor due to the known overestimation of the wavenumbers by this approximation. The usual criteria and theoretical results were taken into account for these assignments. Group wavenumbers

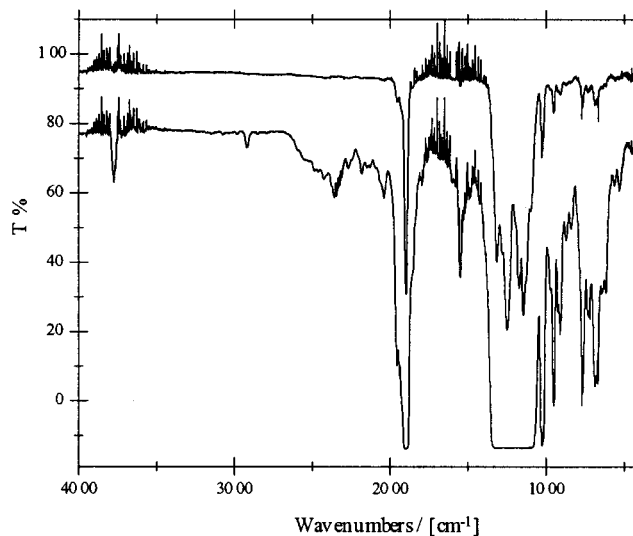


Figure 6. FTIR spectra of $\text{CF}_3\text{OCF}_2\text{OCF}_2\text{C(O)F}$ at room temperature: pressure, 2 and 40 Torr; optical path, 10 cm; resolution, 1 cm^{-1} .

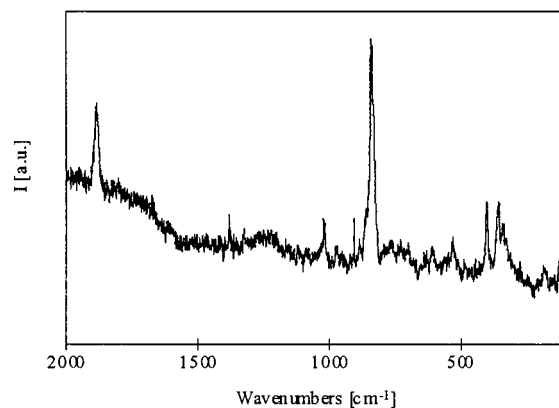


Figure 7. Raman spectrum of the liquid $\text{CF}_3\text{OCF}_2\text{OCF}_2\text{C(O)F}$ at 185 K: excitation line, 514.5 nm (200 mW); resolution, 5 cm^{-1} .

were also considered. Theoretical results allow us to propose the molecular geometry for the main conformer as represented in Figure 5. Theoretical studies also predict the feasibility of rotational equilibrium.

Depending on the symmetry of the rotamers, the normal modes of vibration can be classified for each conformer. For the main conformer, gauche in Figure 5, the $3N - 6 = 39$ normal modes of vibration are all active in infrared and Raman spectra. No splitting was observed for the fundamental bands in either the FTIR or Raman spectra with the exception of the band at 1902 cm^{-1} in the FTIR spectrum. This band could be originated by the C=O stretching vibration of a less stable conformer. The relatively large bandwidths imply rotational isomerism as predicted by the theoretical calculations. Moreover, the most significant differences in the spectra would appear in the region where torsion and deformation modes appear, out of the range of our FTIR spectrometer. The liquid Raman spectrum was taken at low temperature. It increases the concentration of the most stable form and simplifies the spectrum.

A preliminary IR spectrum was reported in a previous paper.¹¹ Table 4 lists the fundamental modes and also combinations and overtones. The most interesting features of these spectra are the C=O stretching band, the C—O—C stretching bands, the C—F stretching, and the CF_3 symmetric deformation, all representative of the structure of this molecule. Thus, the band at 1898 cm^{-1} in the FTIR spectrum can be assigned immediately to the carbonyl stretching. This band is expected to appear at

Table 2. Relative Energies and Torsional Angles of the Stable Conformers of $\text{CF}_3\text{OCF}_2\text{OCF}_2\text{C}(\text{O})\text{F}$ Calculated with Different Theoretical Approximations^a

conformer	HF/3-21G*		HF/6-31+G*		B3LYP/6-31+G*	
	ΔE (kcal/mol)	torsional angles (deg)	ΔE (kcal/mol)	torsional angles (deg)	ΔE (kcal/mol)	torsional angles (deg)
1	0.00	$\tau_1 = -65$ $\tau_2 = 163$ $\tau_3 = 31$ $\tau_4 = 162$ $\tau_5 = 30$	0.49	$\tau_1 = -65$ $\tau_2 = 159$ $\tau_3 = 45$ $\tau_4 = 162$ $\tau_5 = 43$	0.56	$\tau_1 = -64$ $\tau_2 = 160$ $\tau_3 = 47$ $\tau_4 = 167$ $\tau_5 = 47$
2	0.11	$\tau_1 = -64$ $\tau_2 = 161$ $\tau_3 = 153$ $\tau_4 = 37$ $\tau_5 = 39$	0.45	$\tau_1 = -65$ $\tau_2 = 163$ $\tau_3 = 162$ $\tau_4 = 46$ $\tau_5 = 39$	0.51	$\tau_1 = -64$ $\tau_2 = 165$ $\tau_3 = 164$ $\tau_4 = 48$ $\tau_5 = 41$
3	0.26	$\tau_1 = -65$ $\tau_2 = 164$ $\tau_3 = 151$ $\tau_4 = 158$ $\tau_5 = 37$	0.17	$\tau_1 = -65$ $\tau_2 = 163$ $\tau_3 = 159$ $\tau_4 = 160$ $\tau_5 = 43$	0.22	$\tau_1 = -63$ $\tau_2 = 165$ $\tau_3 = 159$ $\tau_4 = 160$ $\tau_5 = 45$
4	0.74	$\tau_1 = -65$ $\tau_2 = 160$ $\tau_3 = 157$ $\tau_4 = -76$ $\tau_5 = 28$	0.24	$\tau_1 = -65$ $\tau_2 = 162$ $\tau_3 = 164$ $\tau_4 = -82$ $\tau_5 = 43$	0.22	$\tau_1 = -65$ $\tau_2 = 164$ $\tau_3 = 166$ $\tau_4 = -80$ $\tau_5 = 45$
5	0.04	$\tau_1 = -67$ $\tau_2 = -163$ $\tau_3 = -155$ $\tau_4 = 38$ $\tau_5 = 37$	0.00	$\tau_1 = -63$ $\tau_2 = -164$ $\tau_3 = -163$ $\tau_4 = 47$ $\tau_5 = 38$	0.00	$\tau_1 = -61$ $\tau_2 = -164$ $\tau_3 = -164$ $\tau_4 = 49$ $\tau_5 = 40$
6	0.70	$\tau_1 = -65$ $\tau_2 = 161$ $\tau_3 = -86$ $\tau_4 = 165$ $\tau_5 = 31$	0.24	$\tau_1 = 65$ $\tau_2 = 163$ $\tau_3 = -83$ $\tau_4 = 165$ $\tau_5 = 43$	0.24	$\tau_1 = -64$ $\tau_2 = 165$ $\tau_3 = -82$ $\tau_4 = 168$ $\tau_5 = 45$
7	1.29	$\tau_1 = -65$ $\tau_2 = 169$ $\tau_3 = -99$ $\tau_4 = -83$ $\tau_5 = 37$	0.71	$\tau_1 = -65$ $\tau_2 = 164$ $\tau_3 = -79$ $\tau_4 = -79$ $\tau_5 = 44$	0.73	$\tau_1 = -65$ $\tau_2 = 167$ $\tau_3 = -75$ $\tau_4 = -75$ $\tau_5 = 46$
8	1.38	$\tau_1 = -177$ $\tau_2 = -168$ $\tau_3 = -34$ $\tau_4 = -87$ $\tau_5 = 38$	1.10	$\tau_1 = -178$ $\tau_2 = -163$ $\tau_3 = -46$ $\tau_4 = -86$ $\tau_5 = 44$	0.92	$\tau_1 = -178$ $\tau_2 = -167$ $\tau_3 = -48$ $\tau_4 = -83$ $\tau_5 = 44$
9	0.88	$\tau_1 = 176$ $\tau_2 = 163$ $\tau_3 = 31$ $\tau_4 = 161$ $\tau_5 = 30$	1.10	$\tau_1 = 178$ $\tau_2 = 159$ $\tau_3 = 45$ $\tau_4 = 162$ $\tau_5 = 43$	0.72	$\tau_1 = 178$ $\tau_2 = 162$ $\tau_3 = 47$ $\tau_4 = 166$ $\tau_5 = 47$
10	0.86	$\tau_1 = 176$ $\tau_2 = 160$ $\tau_3 = 154$ $\tau_4 = 37$ $\tau_5 = 39$	0.82	$\tau_1 = 178$ $\tau_2 = 163$ $\tau_3 = 162$ $\tau_4 = 45$ $\tau_5 = 39$	0.67	$\tau_1 = 177$ $\tau_2 = 165$ $\tau_3 = 163$ $\tau_4 = 47$ $\tau_5 = 41$
11	1.23	$\tau_1 = 173$ $\tau_2 = 163$ $\tau_3 = 151$ $\tau_4 = 157$ $\tau_5 = 37$	0.68	$\tau_1 = 178$ $\tau_2 = 163$ $\tau_3 = 159$ $\tau_4 = 160$ $\tau_5 = 43$	0.42	$\tau_1 = 178$ $\tau_2 = 165$ $\tau_3 = 159$ $\tau_4 = 160$ $\tau_5 = 45$
12	0.69	$\tau_1 = 174$ $\tau_2 = 160$ $\tau_3 = 158$ $\tau_4 = -39$ $\tau_5 = -36$	0.47	$\tau_1 = 178$ $\tau_2 = 163$ $\tau_3 = 163$ $\tau_4 = -47$ $\tau_5 = -38$	0.28	$\tau_1 = 179$ $\tau_2 = 165$ $\tau_3 = 165$ $\tau_4 = -48$ $\tau_5 = -40$
13	0.69	$\tau_1 = -174$ $\tau_2 = -160$ $\tau_3 = -158$ $\tau_4 = 39$ $\tau_5 = 36$	0.47	$\tau_1 = -178$ $\tau_2 = -163$ $\tau_3 = -163$ $\tau_4 = 47$ $\tau_5 = 38$	0.28	$\tau_1 = -179$ $\tau_2 = -166$ $\tau_3 = -165$ $\tau_4 = 49$ $\tau_5 = 40$
14	1.50	$\tau_1 = 176$ $\tau_2 = 160$ $\tau_3 = -84$ $\tau_4 = 166$ $\tau_5 = 30$	0.90	$\tau_1 = -178$ $\tau_2 = -163$ $\tau_3 = -161$ $\tau_4 = -84$ $\tau_5 = 43$	0.59	$\tau_1 = -179$ $\tau_2 = -167$ $\tau_3 = -164$ $\tau_4 = -83$ $\tau_5 = 45$

Table 2 (Continued)

conformer	HF/3-21G*		HF/6-31+G*		B3LYP/6-31+G*	
	ΔE (kcal/mol)	torsional angles (deg)	ΔE (kcal/mol)	torsional angles (deg)	ΔE (kcal/mol)	torsional angles (deg)
15	1.65	$\tau_1 = -176$ $\tau_2 = -161$ $\tau_3 = -153$ $\tau_4 = -84$ $\tau_5 = 35$	0.90	$\tau_1 = -178$ $\tau_2 = -163$ $\tau_3 = -161$ $\tau_4 = -84$ $\tau_5 = 43$	0.59	$\tau_1 = -179$ $\tau_2 = -167$ $\tau_3 = -164$ $\tau_4 = -83$ $\tau_5 = 45$

* $\tau_1 = \text{F1C2C3O4}$, $\tau_2 = \text{C2C3O4C5}$, $\tau_3 = \text{C3O4C5F6}$, $\tau_4 = \text{O4C5O6C7}$, and $\tau_5 = \text{C5O6C7F8}$.

Table 3. Geometrical Parameters for the Most Stable Conformer of $\text{CF}_3\text{OCF}_2\text{OCF}_2\text{C}(\text{O})\text{F}$ (Structure **5** in Table 2) Calculated with Different Theoretical Approximations (Distances in Å, Angles in deg)

param	HF/6-31+G*	B3LYP/6-31+G*
$r(\text{C}_2=\text{O}_9)$	1.1600	1.1828
$r(\text{C}_2-\text{F}_1)$	1.3062	1.3436
$r(\text{C}_2-\text{C}_3)$	1.5330	1.5482
$r(\text{C}_3-\text{O}_4)$	1.3644	1.3880
$r(\text{O}_4-\text{C}_5)$	1.3651	1.3910
$r(\text{C}_5-\text{O}_6)$	1.3548	1.3790
$r(\text{O}_6-\text{C}_7)$	1.3576	1.3834
$r(\text{C}_3-\text{F}_{10})$	1.3227	1.3553
$r(\text{C}_3-\text{F}_{11})$	1.3127	1.3432
$r(\text{C}_5-\text{F}_{12})$	1.3159	1.3482
$r(\text{C}_5-\text{F}_{13})$	1.3081	1.3390
$r(\text{C}_7-\text{F}_8)$	1.3100	1.3404
$r(\text{C}_7-\text{F}_{14})$	1.3082	1.3392
$r(\text{C}_7-\text{F}_{15})$	1.3023	1.3317
$\alpha(\text{F}_1\text{C}_2\text{O}_9)$	124.2	124.0
$\alpha(\text{F}_1\text{C}_2\text{C}_3)$	110.2	109.8
$\alpha(\text{O}_9\text{C}_2\text{C}_3)$	125.6	126.2
$\alpha(\text{C}_2\text{C}_3\text{O}_4)$	106.9	107.0
$\alpha(\text{C}_3\text{O}_4\text{C}_5)$	122.0	121.1
$\alpha(\text{O}_4\text{C}_5\text{O}_6)$	109.7	109.6
$\alpha(\text{O}_6\text{C}_7\text{F}_8)$	112.1	112.6
$\alpha(\text{C}_2\text{C}_3\text{F}_{10})$	109.0	109.0
$\alpha(\text{C}_2\text{C}_3\text{F}_{11})$	110.0	109.7
$\alpha(\text{F}_{10}\text{C}_3\text{F}_{11})$	108.2	107.9
$\alpha(\text{O}_4\text{C}_3\text{F}_{10})$	111.0	111.2
$\alpha(\text{O}_4\text{C}_3\text{F}_{11})$	111.8	112.1
$\alpha(\text{O}_4\text{C}_5\text{F}_{12})$	110.9	111.3
$\alpha(\text{C}_4\text{C}_5\text{F}_{13})$	110.8	111.0
$\alpha(\text{F}_{12}\text{C}_5\text{F}_{13})$	107.8	107.7
$\alpha(\text{O}_6\text{C}_5\text{F}_{12})$	111.2	111.4
$\alpha(\text{O}_6\text{C}_5\text{F}_{13})$	106.2	105.7
$\alpha(\text{O}_6\text{C}_7\text{F}_{14})$	111.3	111.4
$\alpha(\text{C}_6\text{C}_7\text{F}_{15})$	107.0	106.4
$\alpha(\text{F}_{14}\text{C}_7\text{F}_{15})$	108.7	108.7
$\alpha(\text{F}_8\text{C}_7\text{F}_{14})$	108.4	108.3
$\alpha(\text{F}_8\text{C}_7\text{F}_{15})$	109.3	109.3

high wavenumbers due to the influence of the electronegativity of the substituents attached to the carbonyl group: the larger is the sum of the electronegativities of the substituents of the $\text{C}=\text{O}$ group, the higher will be the position of the band in wavenumbers.¹⁶

The $\text{C}-\text{O}-\text{C}$ symmetric and antisymmetric vibrations can be assigned to the FTIR bands at 1180 and 1174 cm^{-1} . The average of these wavenumbers, 1177 cm^{-1} , is higher than that expected for the ether moiety whose values are normally in the range of 1150–1060 cm^{-1} and of 970–800 cm^{-1} .¹⁷ The observed difference is ascribed to the anomeric effect, which reinforces the $\text{C}-\text{O}$ bond in the perfluorinated ether molecule. The influence of the anomeric effect on the $\text{C}-\text{O}$ bond orders of ethers has been elegantly demonstrated by Oberhammer

et al. in their study of CF_3OCH_3 .¹⁸ In that work $\Delta\text{OC} = (\text{O}-\text{C}_\text{H}) - (\text{O}-\text{C}_\text{F}) = 0.079(12)$ Å has been experimentally determined.

The stretching vibrations, involving CF moieties, appear, as expected, in the 1100–1350 cm^{-1} region, starting with the $\text{C}-\text{F}$ stretching vibration at 1147 cm^{-1} until 1316 cm^{-1} where the band originated by the CF_3 antisymmetrical stretching vibration occurs. Interesting enough is the fact that these vibrations are practically inactive in the Raman spectrum of the liquid.

The CF_3 symmetric deformation is another interesting vibrational mode for this kind of molecule, because of its limited range in the vibrational spectra. Thus, this vibration is assigned to the 715 cm^{-1} band in the FTIR spectrum.

Mass Spectra

The interpretation of the mass spectrum is crucial for the determination of the molecular composition of this molecule. Table 5 lists several fragments obtained from the $\text{CF}_3\text{OCF}_2\text{OCF}_2\text{C}(\text{O})\text{F}$ molecule at ionization energies of 20 and 70 eV. There is no doubt about the molecular composition of the compound, due to the identification of all fragments listed in Table 4. M^+ was not detected in the spectrum. This fact is in agreement with the behavior reported for related compounds, for example in the case of $\text{CF}_3\text{OCF}_2\text{C}(\text{O})\text{F}$.¹⁹ The fragment at m/q 201 corresponding to $\text{CF}_2\text{OCF}_2\text{OCF}_3^+$ is detected in the spectra. On the other side of the molecule another signal at m/q 179 is originated by the $\text{FC}(\text{O})\text{CF}_2\text{OCF}_2\text{O}^+$ ion, reinforcing the validation of the proposed structure. Smaller fragments as $\text{FC}(\text{O})\text{CF}_2\text{O}^+$, $\text{OCF}_2\text{OCF}_3^+$, etc., were also observed.

UV–Vis Spectra

The UV–vis spectrum of $\text{CF}_3\text{OCF}_2\text{OCF}_2\text{C}(\text{O})\text{F}$ shows two bands at 208 and 214 nm and a more intense band growing to the 200 nm region, the limit of our spectrometer. It is reasonable to assign this latter band to the $\pi \rightarrow \pi^*$ transition in the $\text{C}=\text{O}$ chromophore. Its position compares very well with that of FCO group in other compounds, like $\text{FC}(\text{O})\text{SCH}_3$,²⁰ with absorption at 198 nm.

Conclusions

$\text{CF}_3\text{OCF}_2\text{OCF}_2\text{C}(\text{O})\text{F}$ was prepared with a yield of 35% by oxidation of C_3F_6 with molecular O_2 using CF_3OF as initiator. The molecular structure was determined by the evaluation of the mass spectrum of the compound, accompanied by the interpretation of the vibrational spectra and that of the UV–visible spectrum.

Due to the inherent difficulty to calculate this molecule using ab initio and density functional theory methods, because of its

(16) Kagarise, R. E. *J. Am. Chem. Soc.* **1955**, *77*, 1377–1379.

(17) Schrader, B. *Infrared and Raman Spectroscopy*; VCH: Weinheim, Germany, 1995; p 209.

(18) Kühn, R.; Christen, D.; Mack, H.-G.; Detlev Kouikowski; Minkwitz, R.; Oberhammer, H. *J. Mol. Struct.* **1996**, *376*, 217–228.

(19) Schack, C. J.; Christe, K. O. *J. Fluorine Chem.* **1979**, *14*, 519–522.

(20) Della Védova, C. O. *J. Raman Spectrosc.* **1989**, *20*, 483–488.

Table 4. Experimental Vibrational Data (IR and Raman) for $\text{CF}_3\text{OCF}_2\text{OCF}_2\text{C}(\text{O})\text{F}$ in cm^{-1} and Theoretical Results Obtained for the Most Stable Form (Structure 5 in Table 2) with Different Approximations

IR ^a	Raman ^a	HF/6-31+G ^{*b,c}	B3LYP/6-31+G [*]	assign
3775				$2 \times 1898 = 3796$
2919				$1898 + 1025 = 2923$
2488				$2 \times 1251 = 2502$
				$1316 + 1174 = 2490$
2475				$1316 + 1174 = 2490$
2462				$1316 + 1147 = 2463$
2427				$1251 + 1174 = 2425$
				$1281 + 1147 = 2428$
2268				$1251 + 1025 = 2276$
				$1316 + 953 = 2269$
				$1174 + 1098 = 2272$
				$1147 + 1128 = 2275$
2244				$2 \times 1128 = 2256$
				$1147 + 1098 = 2245$
2205 sh				$1251 + 953 = 2204$
				$1180 + 1025 = 2205$
2183				$2 \times 1098 = 2196$
				$1174 + 1025 = 2199$
2148				$1128 + 1025 = 2153$
2130				$1174 + 953 = 2127$
2095				$1147 + 953 = 2100$
2068 sh				$1128 + 953 = 2081$
2040				$2 \times 1025 = 2050$
				$1098 + 953 = 2051$
1957				$1281 + 673 = 1954$
1944				$1174 + 774 = 1948$
1925				$1251 + 673 = 1924$
1919				$1147 + 774 = 1921$
1902				
1898 (72)	1887 (36)	1945 (324)	1949	$\nu(\text{C}=\text{O})$
1854				$1098 + 774 = 1872$
1555				
1550				
	1383 (15)	1378 (125)	1328	$\nu(\text{C}-\text{C})$
1316 (55)	1327 (5)	1334 (615)	1289	$\nu_{\text{as}}(\text{CF}_3)$
1281		1306 (323)	1261	$\nu_{\text{s}}(\text{CF}_3-\text{O}-\text{C})$
1261		1280 (923)	1225	$\nu_{\text{as}}(\text{CF}_3)$
1251 (100)		1269 (1021)	1213	$\nu_{\text{as}}(\text{CF}_3)$
1214		1244 (33)	1196	$\nu_{\text{as}}(\text{CF}_2)$
1196		1229 (97)	1170	$\nu_{\text{as}}(\text{CF}_3-\text{O}-\text{C})$
1180		1219 (106)	1161	$\nu_{\text{s}}(\text{C}-\text{O}-\text{C})$
1174 (68)		1171 (662)	1087	$\nu_{\text{as}}(\text{C}-\text{O}-\text{C})$
1147 (79)		1111 (135)	1077	$\nu(\text{C}-\text{F})$
1128				
1098 (34)				
1034				
1029 (20)	1025 (17)	969 (58)	959	$\nu_{\text{s}}(\text{CF}_3)$
1025	1021			
1021				
975	976 (8)			$\nu_{\text{s}}(\text{CF}_2)$
953 (9)				
927				
923				
915				
912 (4)				
907				
	888 (8)			
873	864 (23)	874 (14)	862	$\nu(\text{CF}_3)$
841	845 (100)	834 (5)	821	FCO oop
802 sh				
774 (8)				
768		765 (24)	752	$\delta(\text{FCO})$
750				
745		746 (9)	738	$\delta(\text{COC})$
739				
735	736 (7)			
729				
720 (3)				
715	711 (6)	716 (14)	709	$\delta_{\text{s}}(\text{CF}_3)$
698 sh				
694				
690				

Table 4 (Continued)

IR ^a	Raman ^a	HF/6-31+G ^{*b,c}	B3LYP/6-31+G [*]	assignt
680				
673		673 (103)	667	
668 (7)				
645		630 (0.8)	626	
621	613 (11)	601 (3)	597	
618				
565		567 (11)	563	
533	537 (15)	552 (10)	549	
		521 (21)	518	
	489 (6)	492 (2)	487	
	453 (5)	453 (8)	447	
	408 (29)	396 (0.8)	395	
	364	363 (2)	363	
	343	349 (0.5)	348	
	334	318 (0.9)	315	
	280	291 (0.8)	291	
		233 (5)	233	
	191	202 (0.6)	205	
		161 (1)	163	
		114 (0.8)	119	
		88 (0.1)	91	
		58 (0.3)	57	
		46 (0.5)	43	
		36 (0.3)	35	
		28 (0.1)	29	

^a Between parentheses are relative intensities from the absorption maxima for the most intense bands. ^b Scaled by 0.9 factor. ^c Intensities in km mol⁻¹.

Table 5. Mass Spectra of CF₃OCF₂OCF₂C(O)F

m/q	I _{20 eV}	I _{70 eV}	fragment
201	0.29	0.49	CF ₂ OCF ₂ OCF ₃ ⁺
179	1.71	1.82	FC(O)CF ₂ OCF ₂ O ⁺
151	0.59	0.40	OCF ₂ OCF ₃ ⁺
136	3.28	2.22	¹³ CF ₂ OCF ₃ ⁺ + CF ₂ O ¹³ CF ₃ ⁺
135	100.00	98.28	CF ₂ OCF ₃ ⁺
132	1.16	0.93	CF ₂ OCF ₂ O ⁺
119	0.23	0.51	CF ₂ CF ₃ ⁺
114	0.87	1.82	F ¹³ C(O)CF ₂ O ⁺ + FC(O) ¹³ CF ₂ O ⁺
113	32.65	79.89	FC(O)CF ₂ O ⁺
100	0.11	0.47	CF ₂ CF ₂ ⁺
97	0.73	1.61	FC(O)CF ₂ ⁺
91	<0.1	0.50	FC(O) ⁺ + CO ₂ ⁺ ?
85	0.35	7.23	OCF ₃ ⁺
81	<0.1	0.52	C ₂ F ₃ ⁺ ?
70	0.37	2.41	¹³ CF ₃ ⁺
69	28.19	100.00	CF ₃ ⁺
67	<0.1	0.25	O ¹³ CF ₂ ⁺
66	0.93	11.87	OCF ₂ ⁺
50	<0.1	6.53	CF ₂ ⁺
48	<0.1	0.93	F ¹³ C(O) ⁺
47	5.52	64.80	FC(O) ⁺
44	<0.1	1.59	CO ₂ ⁺
31		1.70	CF ⁺

five torsions, a smaller molecule was used as a model. Then, CF₃OCF₂C(O)F was fully calculated at the HF/3-21G^{*} level of the theory. The five minima were subsequently calculated at the HF/6-31+G^{*}, B3LYP/6-31+G^{*}, and B3PW91/6-31+G^{*} levels. The two most stable conformations were used for further calculations of CF₃OCF₂OCF₂C(O)F. A chain structure is predicted as the most stable form. Most of the 15 calculated

conformers fall in the range of 1 kcal/mol, demonstrating the high conformational flexibility of this molecule. The two most stable forms are those with the structures making maximum the anomeric effect.

This molecule provides a useful model compound to study the properties of other more complex perfluoro polyethers whose important applications are described elsewhere.

Acknowledgment. The authors thank Mr. Z. Czarnowski for very helpful comments. This work was financially supported by the Consejo Nacional de Investigaciones Científicas y Técnicas. C.O.D.V. and R.M.R. thank the Fundación Antorchas (República Argentina), Alexander von Humboldt Stiftung, the British Council, and DAAD (Deutsche Akademische Austauschdienst of Germany) for financial support and for the DAAD–Fundación Antorchas and Alexander von Humboldt Stiftung–Fundación Antorchas Awards for German–Argentine cooperation and the British Council–Fundación Antorchas award for British–Argentinean cooperation. They also thank the Consejo Nacional de Investigaciones Científicas y Técnicas (CONICET) (PIP 4695), Agencia Nacional de Promoción Científica y Tecnológica (PICT 122), and Comisión de Investigaciones Científicas de la Provincia de Buenos Aires (CIC), República Argentina, for financial support. They are indebted to the Facultad de Ciencias Exactas, Universidad Nacional de La Plata, República Argentina, for financial support and to Fundación Antorchas for the National Award for Argentinean cooperation.

IC0008520